HHS Public Access

Author manuscript

Cancer Gene Ther. Author manuscript; available in PMC 2012 December 01.

Published in final edited form as:

Cancer Gene Ther. 2012 June ; 19(6): 431–442. doi:10.1038/cgt.2012.21.

Pharmacokinetic study of neural stem cell-based cell carrier for oncolytic virotherapy: Targeted delivery of the therapeutic payload in an orthotopic brain tumor model

Bart Thaci[1,3], **Atique U. Ahmed**[1,3], **Ilya V. Ulasov**[1], **Alex L. Tobias**[1], **Yu Han**[1], **Karen S. Aboody**[2], and **Maciej S. Lesniak**[1,*]

[1]The Brain Tumor Center, The University of Chicago, Chicago, Illinois, USA

[2]Department of Neuroscience, City of Hope National Medical Center and Beckman Research Institute, Duarte, California, USA

Abstract

Oncolytic virotherapy is a promising novel therapy for glioblastoma that needs to be optimized before introduced to clinic. The targeting of conditionally replicating adenoviruses (CRAds) can be improved by relying on the tumor tropic properties of neural stem cells (NSCs). Here, we report the characterization of an FDA approved NSC, HB1.F3-CD, as a cell carrier for CRAd-S-pk7, a glioma-tropic oncolytic adenovirus. We show that NSCs replicate and release infectious CRAd-S-pk7 progeny capable of lysing glioma cell lines. Moreover, *ex-vivo* loaded NSCs, injected intracranially in nude mice bearing human glioma xenografts (i) retained their tumor-tropism, (ii) continued to replicate CRAd-S-pk7 for more than a week after reaching the tumor site and (iii) successfully handed-off CRAd-S-pk7 to glioma cells *in vivo*. Delivery via carrier cells reduced non-specific adenovirus distribution in the mouse brain. Moreover, we assessed biodistribution of loaded NSCs after intracranial injection in animal models semi-permissive to adenovirus replication, the Syrian hamster and cotton rat. NSCs did not migrate to distant organs and high levels of CRAd-S-pk7 DNA were observed only in the injected hemisphere. In conclusion, this optimized carrier system, with high efficiency of adenovirus delivery and minimal systemic toxicity, poses considerable advantages for anti-glioma oncolytic virotherapy.

Keywords

neural stem cell; carrier; oncolytic virus; adenovirus; hamster; cotton rat

[*]To Whom Reprint Request Should Be Addressed: The Brain Tumor Center, The University of Chicago Pritzker School of Medicine, 5841 South Maryland Ave, M/C 3026, Chicago, IL 60637; Tel (773) 834-4757; Fax (773) 834-2608, mlesniak@surgery.bsd.uchicago.edu.

[3]These authors contributed equally to this work

Conflict of Interests/Disclosure

Karen Aboody is CSO and Director of TheraBiologics, Inc. All other authors declare no conflict of interest.

Supplementary information is available online at the Cancer Gene Therapy website.

Introduction

Glioblastoma (GBM) is the most common primary brain tumor and portends the worst prognosis among all central nervous system (CNS) malignancies[1]. The mean overall survival (OS) has only slightly improved over the last 30 years[2]. The current standard of care relies on surgical resection, fractionated radiotherapy and chemotherapy[3]. The therapeutic efficacy of most of these treatment modalities is limited due to the invasive nature of the tumors. By the time gliomas are diagnosed they have already infiltrated diffusely and thus are extremely difficult for complete surgical resection therefore limiting the benefits of gross total removal. The low oxygen level in the glioma environment negatively affects radiotherapy[4]; while cellular heterogeneity and glioma stem cells account for the emergence of resistance to therapeutic regimens[5, 6]. Therefore, there is an urgency to develop novel therapies capable of overcoming the common resistance mechanisms of gliomas[7].

One such therapy involves harnessing oncolytic viruses to kill glioma cells. The concept of exploiting viruses, for their oncolytic potential, has a century-old history, but only within the last 20 years has this approach been considered for the treatment of brain tumors[8]. Our lab has been focused on conditionally replicating adenoviruses (CRAd) due to their proven efficacy in preclinical glioma models[9]. CRAd-S-pk7, the vector that we intend to bring into clinical trials, consists of two genetic modifications: i) a fiber modification containing polylysine that binds with high affinity to heparan sulfate proteoglycans and ii) E1A transcription under the control of survivin promoter[9–11]. These modifications provide CRAd-S-pk7 the necessary tumor specificity allowing for selective replication in glioma cells and minimal toxicity to normal brain tissue[9]. Furthermore, CRAds have the capacity to kill different subsets of glioma cells without being confined to the resistance of conventional therapies.[12]. Therefore, they hold a great promise in the armamentarium against gliomas.

There have been at least six formal clinical trials using oncolytic viruses to treat malignant brain tumors[13, 14]. Despite some degree of therapeutic efficacy shown in these clinical trials, overall, they have fallen short of expectations. Most oncolytic viral therapies, including CRAd, face some challenges before they can be translated into the clinic. Issues pertaining to the successful clinical translation of oncolytic virotherapy for gliomas are: i) the limited distribution of viral vectors after intratumoral injection, ii) the immune clearance induced shortly after injection, and iii) the inability of the currently available vectors to target disseminated tumor burdens. To overcome these hurdles, cell carriers have been used to improve targeting and distribution while reducing the immune response towards viral vectors[15–17]. Numerous carrier cell/oncolytic virus combinations are currently under investigation[18, 19]. Each represents a unique biotherapeutic system with different kinetics of therapeutic virus replication, *in vivo* tumor homing ability and thus must be examined extensively.

Our laboratory along with others is actively pursuing the development of a stem cell-based carrier system for anti-glioma oncolytic virotherapy. Recently, we have shown neural stem cell (NSC) carriers to be superior to mesenchymal stem cells (MSCs) in delivering CRAd-S-pk7 to orthotopic glioma models and therefore NSCs enhance the therapeutic potential of

oncolytic virotherapy[18]. To progress to a clinical trial, it is necessary to characterize and quantify the pharmacokinetic properties of NSCs as cell carriers. Here, we report a thorough characterization of a Food and Drug Administration (FDA) approved immortalized neural stem cell line (HB1.F3-CD) as an effective cell carrier for CRAd-S-pk7[20]. First, we provide evidence of the NSC's potential of replicating and releasing infectious progeny that can kill glioma cell lines. Then, we show that, in nude mice bearing orthotopic human glioma, NSCs do not alter their inherent tumor tropic properties post infection and produce infectious virus progeny for more than a week after reaching the tumor site. Furthermore, we observed that the NSC-based cell carrier significantly reduced the non-specific therapeutic virus distribution in the animal brain. Finally, to better characterize the systemic biodistribution of adenovirus after intracranial injection of NSCs loaded with CRAd-S-pk7, we utilized cotton rats and hamsters, two pre-established semi-permissive animal models. We show that carrier cells do not disseminate to distant organs and high titers of infectious progeny are present only at the injected hemisphere. Thus, the unique tumor-tropic properties of neural stem cells combined with an improved safety profile of intracranial adenovirus injection brings this cell-carrier based anti-glioma oncolytic virotherapy one step closer to clinical trials.

Material and methods

Cell Lines and Vectors

HB1.F3-CD is a *v-myc* immortalized human NSC (hNSC) line, derived from the human fetal brain that constitutively expresses cytosine deaminase (CD)[20]. NSCs were maintained as adherent cultures in DMEM supplemented with 10% fetal bovine serum (FBS) (Atlanta Biologicals, Lawerenceville, GA, USA), 2 mmol/l L-glutamine, 100 units/ml penicillin, 100 ug/ml streptomycin and 0.25 ug/ml amphotericin B (Invitrogen, Carlsbad, CA, USA). U87MG, U251MG, U118MG and A549 carcinoma cell lines were purchased from American Type Culture Collection (ATCC, Manassas, VA, USA); while N10 glioma was purchased from the Japanese Tumor Tissue Bank (Tokyo, Japan). All cells were grown in minimal essential medium (MEM) with 10% FBS, 100 μg/ml penicillin and 100 μg/ml streptomycin.

The replication competent adenoviral vector CRAd-S-pk7 harbors two genetic mutations:[9, 11] a) fiber modification was achieved by insertion of 7 poly-Lysine repeats (pk7) in the C-terminal of knob domain; while b) human survivin promoter drives expression of the E1A region.

Generation of green fluorescent protein (GFP) *or* firefly luciferase (Fluc) *expressing HB1.F3-CD*

In order to detect the distribution of NSCs *in vivo* we generated a GFP and Fluc expressing HB1.F3-CD. GFP expressing cells were infected with a replication-incompetent retroviral construct; while for Fluc we infected cells with a replication-incompetent lentiviral vector, as described in detail elsewhere[17]. We used 4 μg/ml puromycin in DMEM media to isolate stable expressing clones.

Antibodies and other reagents

For flow cytometer, cells were stained with mouse anti-human CAR (Abcam, Cambridge, MA, USA), CD138, αvβ3, αvβ5 (Ebioscience, San Diego, CA, USA) and rat anti-human perlecan; followed by AlexaFluor647 (Invitrogen) conjugated secondary antibodies. Adenovirus transduced cells were detected using a goat anti-Hexon FITC conjugated antibody (Millipore, Billerica, MA, USA). For immunofluorescence, FITC conjugated anti-GFP antibody, biotin conjugated anti-hexon and FITC-conjugated Ig control were purchased from Abcam; human CD44 rabbit monoclonal antibody purchased from Epitomics (Burlingame, CA, USA); AlexaFluor555-Streptavidin and Alexafluor350 donkey anti-rabbit from Invitrogen.

Flow Cytometry

For detection of surface receptors, cells were detached using trypsin/EDTA and stained with primary antibodies for 1 hour at 4°C, followed by secondary antibodies for 30 minutes at 4°C. For quantification of adenovirus transduction of HB1.F3-CD, 48 hours after infection, cells were detached, washed with PBS and then permeabilized with a methanol/acetone solution (as per Millipore protocol) before staining with FITC-conjugated goat anti-Hexon. Cells were analyzed using a BD FACSCanto cytometer and graphs were rendered using FloJo software.

Cell viability assays

NSC and glioma viability was determined using the MTT cell proliferation kit (Roche Diagnostics, Mannheim, Germany). Briefly, in a 96-well plate we plated 3000 cells/well, the day before infection. NSCs were infected with different concentrations of CRAd-S-pk7; instead glioma cells were incubated with the supernatant of previously infected NSCs. Viability was determined three days later, as described by the manufacturer's protocol.

Viability of glioma cells after incubation with the supernatant of previously infected NSCs was also assessed via crystal violet. NSCs were infected earlier with CRAd-S-pk7 at different concentrations 1, 10, 50 and 100 infectious units per ml (IU/ml). Five days later the supernatant was collected and used to infect glioma cell lines and A549 carcinoma plated in 24-well plates. Three days later viability was determined. Shortly after aspirating the media the cell layer was covered with the crystal violet solution (1%) and incubated for 20 minutes at room temperature. Then wells were washed carefully and let dry at room temperature. Images were taken with an inverted microscope.

Determination of adenoviral E1A copies via quantitative PCR

Total DNA from cultured cells or animal tissues was extracted using DNeasy Tissue Kit (Qiagen, Valencia, CA, USA). Adenoviral E1A gene expression was quantified via quantitative real-time PCR using iQ™ SYBR green supermix (Bio-Rad, Hercules, CA, USA), using primers described elsewhere[21]. For each animal model we generated separate standard curves of E1A copies containing 100ng DNA. The sensitivity of this assay was set to detect as low as 5 E1A copies per 100ng DNA (Supplementary Figure S1). All samples were run in triplicates using an Opticon2 system (Bio-Rad). Results are expressed as E1A copy number per 100ng DNA.

Immunohistochemistry

For immunohistochemistry (IHC), brains were sectioned in 10 μm thick sections. After thawing, sections underwent fixation/permeabilization with a solution of 50/50 acetone-methanol, at −20°C for 5 minutes. Then, the slides were washed with ice-cold phosphate-buffered saline (PBS) and blocked with 10% BSA for 30 minutes. We incubated overnight at 4°C with primary antibodies and 1 hour at room temperature with the secondary antibody. After washing the excess antibody, slides were mounted with Prolong® Gold antifade reagent with DAPI (Invitrogen). Fluorescent images were documented with an inverted Axiovert200 Zeiss microscope.

In vivo tracking of NSCs with bioluminescence imaging

For *in vivo* tracking of NSC migration to the tumor, we relied upon photonflux imaging[17]. Mice were imaged for Fluc activity following intraperitoneal injection of D-luciferin (4.5 mg/animal in 150 μl saline), and photon counts were recorded 10 minutes after D-luciferin administration by using a cryogenically cooled high-efficiency charged-coupled device camera system (Xenogene).

Determination of adenoviral progeny titers

For quantification of the infectious progeny released or inside the NSCs, the supernatant and cell mass were collected separately. Cells were resuspended in 200 μl of PBS and freeze-thawed three times to release the viral progeny. Then, the supernatant and the cell suspension were centrifuged for 5 minutes at 4000rpm to spin down the cell debris and 20 μl from each sample were used to infect a confluent layer of 293-HEK (Human Embryonic Kidney) cells, as per Adeno Rapid-X Titer Kit protocol (Clontech, Mountain View, CA, USA). 48 hours later the cell layer was fixed/permeabilized with methanol and stained for hexon plaques. Infectious units (i.u./ml) values quantified through this protocol are similar to plaque forming units (Pfu).

For determination of adenoviral titers in animal organs, the tissue was collected at the time points indicated, resuspended in PBS to provide a concentration of 1 μg/μl and then homogenized. For each sample, the same amount of tissue, in 50 μl, was freeze-thawed three times, the debris was spun down and 20 μl were used to infect 293-HEK cells, as above. Instead, for determination of circulating infectious viral progeny titers in animals, we analyzed their serum by using the same protocol.

Detection of v-myc positive NSCs via nested PCR

We relied on a 2 step nested PCR to detect presence of *v-myc* in animal tissues. In the first step, a 588 base pair (bp) region from the v-myc gene was amplified using forward primer 5'-CCTTTGATTTCGCCAAT-3', reverse 5'-GCGAGCTTCTCCGACACCACC-3'. By using 1μl from the first PCR and a second pair of primers: forward 5'-TCACAGCCAGATATCCAGCAGCTT-3', reverse 5'-ACTTCTCCTCCTCCTCCTCG-3' we amplified a 166 bp sequence from the *v-myc* gene. As a DNA loading control we used a house-keeping gene, GAPDH: forward primer 5'-CATTGACAACTACAT-3' and reverse 5'-TCTCCATGGTGGTGAAGAC-3', to amplify a 220bp sequence. The sensitivity and

specificity was determined by spiking animal DNA with different dilutions of human neural stem cells DNA (Supplementary Figure S2). PCR products were resolved on a 2% agarose gel, stained with ethidium bromide, and bands were quantified using the Chemidoc Gel documentation system (Bio-Rad).

Ex vivo loading

The total number of cells to be injected *in vivo* was based on our previous studies, where we reported that infection with 50 i.u./cell of CRAd-S-pk7 virus resulted in maximum progeny released over time with minimum toxicity to carrier cell and proved superior survival benefit to glioma bearing mice[17, 18]. In order to optimize the *ex vivo* loading protocol, we first examined infection efficiency of CRAd-S-pk7 virus. For this, cell suspension and monolayer of HB1.F3.CD cells were incubated with DMEM (10% FBS) containing 50 i.u./cell CRAd-S-pk7 virus for 1, 2 and 4 hours. Infected cells were than washed and cultured for 24 hours. Cells were than harvested and subject to FACS analysis with goat anti-Hexon FITC conjugated antibody (Millipore) and measurement of viral DNA replication by PCR method as described previously.

Animal experiments

Animals were cared for according to a study-specific animal protocol approved by The University of Chicago Institutional Animal Care and Use Committee. Intra-cranial (IC) engraftment, distribution and survival of HB1.F3.CD-GFP loaded or not with CRAd-S-pk7 were studied in normal mouse and hamster brains and in the presence of orthotopic U87 human glioma xenografts in nude mice. In brief, seven to eight-week-old male nude mice (Harlan Laboratories, Madison, WI, USA) were anesthetized with an IP injection of ketamine hydrochloride (25 mg/ml)/xylazine (2.5 mg/ml) cocktail. For IC injection, a midline incision was made, and a 1-mm burr hole centered 2 mm posterior to the coronal suture and 2 mm lateral to the sagittal suture was made. Animals were placed in a stereotactic frame and injected with a 26 Gauge Hamilton needle 2×10^5 U87 cells or PBS, in 2.5μl volume, 3 mm deep into the brain. Twenty-one days after tumor implantation, mice were injected IC, using the same burr hole as above, with 5×10^5 HB1.F3.CD-GFP loaded or not with 50 i.u./cell of CRAd-S-pk7.

For determination of HB1.F3.CD-GFP cell viability after IC injection, mice were sacrificed at the described time points. Their brains were snap-frozen in a mixture of 2-N-methyl-bromide and methyl-butane; then cut coronally at the injection site in 2 pieces and embedded in OCT in a dry ice-methylbutane bath. Sections of 10 μm, spanning approximately 2 mm of tissue, were stained with the described antibodies. The selection criteria for high power field (HPF) were based on quantifying those areas with the highest number of HB1.F3.CD-GFP cells. That meant counting GFP positive cells at the injection site in normal mouse brains; while in glioma bearing mice we counted cells on the tumor-normal brain interface. The mean number of GFP (+) positive per HPF (630X) was plotted to compare between different groups.

Four to five week-old male hamsters (Harlan Laboratories) were anesthetized with an intramuscular (IM) injection of ketamine hydrochloride (25 mg/ml) and injected IC as above

with 5×10^5 HB1.F3-CD-GFP loaded or not with 50 i.u./cell of CRAd-S-pk7, 5 mm deep into the brain. Hamsters were sacrificed on day 1, 7 and 30; then brains were processed as above.

Intracranial CRAd-S-pk7 replication delivered by direct injection or loaded onto carrier cells, HB1.F3-CD, was quantified via qRT-PCR and titer assay. Three weeks after injecting 2×10^5 U87 cells IC, we injected in the same location either 2.5×10^7 i.u. CRAd-S-pk7 per animal or 5×10^5 HB1.F3-CD loaded with 50 i.u./cell of CRAd-S-pk7. Animals were sacrificed 4, 7 and 14 days later; their brain hemispheres separated, then homogenized. Viral replication was quantified via qPCR for adenoviral E1A and by using AdenoX titer kit for progeny.

Systemic distribution and replication of CRAd-S-pk7 delivered IC by HB1.F3-CD carrier cells, was studied in hamsters and cotton rats. Cotton rats were anesthetized with an intraperitoneal (IP) injection of ketamine hydrochloride (25 mg/ml)/xylazine (2.5 mg/ml) cocktail, while hamsters underwent the same procedure as above. 5×10^5 HB1.F3-CD cells loaded or not with 50 i.u./cell of CRAd-S-pk7 were injected per animal. Animals were sacrificed at the indicated time points and their brain hemispheres separated (the injected right hemisphere vs. left hemisphere). To quantify systemic adenovirus distribution, we harvested serum, lungs, kidneys, liver and spleen from each animal. All tissues were weighed; the same amount of PBS (μl) per μg tissue was added and then homogenized. Total DNA was isolated form animal tissues using DNeasy Tissue Kit (Qiagen). Adenoviral E1A gene expression was quantified by quantitative real-time PCR using iQ™ SYBR green supermix from Bio-Rad (Hercules, CA). All samples were run in triplicates using an Opticon2 system (Bio-Rad). Results are expressed as E1A copy number per 100ng DNA. Adenoviral titers in animal's tissues and serum (Table 1) were determined.

Statistical analysis

The statistical analysis presented was performed using GraphPad Prism Software, v4.0 (GraphPad Software, La Jolla, CA). Where applicable, a standard independent two-sample *t*-test was applied. A P value <0.05 was considered statistically significant (***P value <0.001; **P value <0.01; *P value <0.05).

Results

Permissiveness of HB1.F3-CD neural stem cell carrier for CRAd-S-pk7 infection

The ultimate goal of *ex-vivo* loading is to effectively infect as many carrier cells as possible. Thus, to evaluate the permissiveness of NSC to CRAd infection, we first examined the expression of adenovirus cell attachment and internalization receptors in NSCs (Figure 1a). Although NSCs expressed minimal levels of the adenovirus primary attachment receptor CAR, about 50% of NSCs expressed CD138, one of many heparan sulfate proteoglycans that can function as a primary binding receptor. Also, 91% of NSCs expressed the $\alpha_v\beta_5$ internalization receptor.

In order to establish an optimal loading dose for in vivo delivery, an MTT assay was performed to evaluate the toxicity induced by CRAd-S-pk7 virus during this process (Figure

1b). At the low dose (1–10 i.u./cell) CRAd-S-pk7 did not induce toxicity to NSCs. However, the viability was reduced about 25% at the dose of 50 i.u./cell and about 50% when NSCs were infected with 100 i.u./cell.

Next, to establish the replication kinetics of CRAd-S-pk7 in NSCs, we infected/loaded them with varying concentrations of CRAd. As shown in Figure 1c, the viral DNA replication at day 3 was highest when loaded with 50 i.u./cell, amounting to 1.6×10^6E1A copies/ngDNA. At this loading dose, the viral burst size was about 5 and 2-fold larger than the loading dose of 1 and 10 iu/cell respectively (**p=0.002 and *p=0.024). When NSCs were loaded with 100 i.u./cell, the CRAd-S-pk7 DNA replication did not improve significantly as compared to 50 i.u./cell (*p=0.56*), and NSC viability was significantly reduced at this level. Combining toxicity data along with DNA replication data, a loading dose of 50 i.u./cell was selected to further evaluate NSCs as a carrier system for oncolytic virotherapy. At this loading dose, viral DNA replication continued to increase up to 7 days post infection (Figure 1d).

Our next objective was to establish an optimal exposure time in order to achieve maximum infectivity/loading, while minimizing oncolytic virus mediated toxicity. We measured adenovirus transduction rate by analyzing Ad-hexon expression and viral DNA replication after varying CRAd-S-pk7 incubation times with both HB1.F3-CD adherent monolayer and suspension cells (1–4 hours). After incubating NSCs in suspension at the loading dose of 50 i.u./cell for 2 hours, a maximum loading /infection of the CRAd-S-pk7 was achieved (**p=0.002) (Figure 1e, f). Based on these data, we decided to load/infect NSCs in suspension at the loading dose of 50 i.u./cell for 2 hours for our future experiments.

HB1.F3-CD loaded with CRAd-S-pk7 produces infectious progeny and induces glioma cell oncolysis

To assess the ability of this carrier system to produce infectious adenoviral progeny, we incubated tumor cells with the supernatant of previously infected HB1.F3-CD cells. At day 5 post infection the intracellular virus titer reached its maximum. At day 7 post infection, the intracellular viral titer decreased as the titer of the cell-free viral progeny reached its maximum level, indicating that it takes about 5–6 days for the CRAd-S-pk7 to complete its life cycle in the HB1.F3.CD carrier system (Figure 2a).

Next, to evaluate the oncolytic capacity of the viral progeny released from CRAd-S-pk7 infected NSCs, a panel of four human glioma cell lines was exposed to the supernatant of NSCs loaded/infected with various doses of CRAd-S-pk7 for 120 hours. Figure 2b is a pictorial representation of tumor cell toxicity produced by the therapeutic viral progeny from infected HB1.F3-CD cells. Regardless of the loading dose, the released CRAd-S-pk7 viral progeny was able to induce tumor cell killing in all tested glioma cell lines at day 3 post incubation (Figure 2c). As compared to the tested glioma cell lines, NSC carrier cells were much more resistant to CRAd-S-pk7 mediated oncolysis (Figure 1b, 2c) [18].

Distribution of the CRAd-S-pk7 loaded HB1.F3-CD carrier cells in nude mouse brains

The intrinsic tumor homing properties of NSCs are the key attribute to their utility as a cell carrier for oncolytic virotherapy. Therefore, it is of paramount importance to examine how

adenovirus loading affects the engraftment, distribution and survival of the implanted NSC in the animal brain. In order to monitor the implanted stem cell distribution effectively, the HB1.F3-CD cells were further modified to express GFP by using a replication incompetent retroviral vector, as described in Material and Methods. 5×10^5 NSCs loaded with or without the CRAd-S-pk7 virus (50 i.u./cell) were stereotactically implanted in the brains of nude mice. Viability and distribution of NSCs were assessed at the indicated time points (1, 5, 12 and 17 days post NSC implantation) via immunohistochemistry. On day 1 (Figure 3a), a majority of the implanted cells were localized and clumped together at the injection site. On day 5, the clumping was significantly reduced and most of the cells were located at the implanted site. Most importantly, CRAd-S-pk7 loading appeared to have had minimal or no effect on the viability of the carrier cell as measured by the number of GFP positive HB1.F3-CD cells present in the section of animal brains at day 5 and day 12 post implantation (Figure 3b). Also to be noted: NSCs were not detectable in the contralateral hemisphere (NSCs were implanted on the right side). At day 17 of post implantation, the NSCs were undetectable in animal brains via immunohistochemical analysis.

Distribution of CRAd-S-pk7 loaded HB1.F3-CD in nude mouse brain bearing orthotropic U87 human glioma xenograft

Next, the adenovirus loading effects on the NSCs' engraftment, distribution and survival, were examined in the animal brain bearing a human glioma xenograft. On day 1, the distribution was very similar to the animal brain without any tumor as cells clumped at the injection site (Figure 4a). On day 5, implanted cells were distributed around the tumor (Figure 4a, b). Again, we did not observe any NSCs migrating to the hemisphere contralateral to the implanted hemisphere. The total number of NSC-GFP positive cells that surrounded the U87 xenograft did not differ between infected vs. non-infected NSC, showing no difference in cell survival (Figure 4c). After 12 days post implantation, the viability of NSCs drops to 1 NSC/hpf (high power field) for both infected and non-infected and became undetectable at 17 days post implantation. Taken together, we conclude that loading oncolytic virus into NSCs had a minimal effect on their viability and engraftment capacity *in vivo*.

In vivo delivery of the therapeutic CRAd-S-pk7 virus by the HB1.F3-CD carrier cell

To assess the clinical relevancy of our carrier-based oncolytic virotherapy, we next investigated virus hand off ability and the intracranial distribution of the therapeutic virus *in vivo*. The HB1.F3-CD cells infected with CRAd-S-pk7 virus were implanted in the brain of nude mice bearing U87 human xenograft tumor as described previously. Mice were sacrificed at days 1 and 5 post implantation and animal brains were subject to immunohistochemical analysis for GFP (carrier cell specific) and adenoviral hexon protein. As shown in Figure 5a, implanted carrier cells were clumped together at the injected site at 24 hours post implantation. At 5 days post implantation, the carrier cells surrounded the tumor and, most importantly, the GFP negative tumor cells were positive for hexon staining (Figure 5a, right panel, arrows). Taken together, these data indicate that carrier cells loaded with CRAd-S-pk7 are able to hand off the therapeutic virus to their surrounding tumor cells.

Glioma foci/microsatellites can be located further away from the initial implanted site of the therapeutic NSC and loaded NSCs will have to migrate longer distances before delivering the payload. To examine whether CRAd loaded HB1.F3.CD can migrate to disseminated tumor foci and deliver the therapeutic payload effectively, we first established HB1.F3.CD cells stably expressing F-luciferase (Luc) gene by lentivirus-mediated transduction. We then loaded the HB1.F3.CD-Luc cells with 50 i.u. per cell of CRAd-S-pk7 and implanted the cells in the contralateral hemisphere of the U87 xenograft containing animals (Figure 5b). As shown in Figure 5c with bioluminescence imaging, at 72 hours post implantation adenovirus loaded HB1.F3-CD.Fluc cells were able cross the midline and migrate to the contralateral hemisphere. Animals were sacrificed and brain tissue was subject to immunohistochemical analysis for adenovirus hexon positive HB1.F3.CD cells in the U87 tumor foci stained with human specific anti-CD44 antibody (Figure 5d-ii). We observed Ad hexon positive cells in the xenograft tumor foci located in the contralateral hemisphere indicating that implanted CRAd loaded HB1.F3.CD cells were able to migrate to the distance tumor foci and deliver the therapeutic payload (Figure 5d i–iii).

Carrier cell delivery reduces off-site levels of adenoviral titers

Next, we evaluated intracranial distribution of CRAd-S-pk7 post implantation, either of the naked virus or virus loaded HB1.F3-CD cell carrier, in a nude mice brain bearing human glioma xenografts. Five animals from each group were sacrificed at 4, 7 and 14 days post implantation and were subject to viral distribution analysis by examining the presence of the viral DNA as well as infectious progeny. As shown in Figure 6a, the amount of infectious viral particles recovered from both the injected and the contralateral hemisphere of the animal brains that received naked CRAd-S-pk7 virus was very similar. On the other hand, when the therapeutic virus was delivered loaded into carrier cells, the viral distribution was more robust (about 2-log greater) and localized at the injected hemisphere (Figure 6b) as compared to the contralateral hemisphere (**$p<0.01$). As shown in Table 1, the infectious viral progeny was recovered in two out of five animal brains from the contralateral non-injected hemisphere (Figure 6d) as compared to all five animals in the virus alone group (*$p<0.05$).

Evaluation of intracranial viral distribution in the semi-permissive cotton rat and hamster model

To examine the adenovirus replication in immunocompetent semi-permissive hosts, cotton rat and hamster animal models, a previously established quantitative real-time PCR (qRT-PCR) protocol was utilized to monitor viral DNA copies over time[21]. In both hamster and cotton rat models, adenoviral replication was predominately localized at the injection site (right hemisphere) and over time the viral replication gradually decreased to less than 100 copies of E1A (Figure 7a). The recovered adenoviral E1A copies on the non-injected left hemisphere were about 2-log lower as compared to the injected site. Moreover, we could detect infectious progeny only from the injected right hemisphere (Table 1). The liver was the only organ outside of the brain where viral replication was detectable up to 7 days post implantation. In other organs, viral DNA was only detectable at 24 hours post implantation. Additionally we did not detect any infectious progeny in hamster or cotton rat sera (Table 1). To investigate whether loaded NSCs were migrating away from the original injection

site, we relied on a highly sensitive, nested PCR based method that could detect DNA from a single HB1.F3-CD cell in 100 ng of host DNA (Supplementary Figure S2). By using this method we were able to detect HB1.F3-CD specific *v-myc* PCR signal in the implanted right hemisphere of the brain in both of the animal models (Figure 7b, c and Supplementary Figures 3a, b). The HB1.F3-CD signals were only detectable at 24 hours post implantation. HB1.F3-CD distribution in the tissue of implanted brains was very similar to what we observed in the nude mice experiments. Both CRAd loaded and unloaded HB1.F3-CD cells were predominately found clumping together at the injected sites after 1 day of implantation (Figure 7d). However, we could not identify any viable HB1.F3-CD cells at 7 days post implantation. Taken together, we observed that carrier cells were only detectable in the implanted hemisphere of the animal brains at 24 hours post implantation.

Discussion

Virus-infected cells can serve as delivery vehicles to improve adenovirus distribution in tumors, hide the virus from the host immune system and act as *in situ* virus producing factories that generate oncolytic virus progeny at the tumor beds. Specifically, cells with inherent tumor tropic properties are a very attractive candidate for the anti-glioma oncolytic virotherapy carrier system. Neural stem cells constitute one such carrier system that has demonstrated unique tropism towards brain neoplasia in animal models. This phenomenon was shown first by Aboody and colleagues, who used engrafted immortalized NSCs, HB1.F3-CD, to selectively deliver therapeutic agents to invasive satellite tumors[22]. In the last decade many studies have shown that NSCs expressing/carrying the therapeutic payload have anti-glioma activity and based on these promising results, the FDA has recently approved the HB1.F3-CD immortalized stem cell line for a clinical trial[23].

Our lab was one of the first to study the advantages of using stem cells as carriers for oncolytic adenoviruses. In that regard, we have studied the carrier properties of both MSCs and NSCs[15, 16]. We found that both of these carrier systems can be loaded with adenovirus and increase its distribution to the tumor site by acting as micro-factories for virus replication. Also, we have shown that stem cell carrier systems not only hide the payload from the immune system but also have the capability to suppress anti-viral innate immune responses[18, 24]. This allows for enhanced dissemination, increased persistence of adenovirus and can result in enhanced therapeutic benefits. Moreover, we recently demonstrated that delivery of oncolytic adenovirus in the orthotropic human glioma xenograft model via NSCs can improve the median animal survival by ~50%[17]. Nevertheless, such carrier systems need to be optimized before undergoing clinical testing.

Any new therapeutic intervention must go through rigorous pharmacological evaluation before it can translate into a clinical setting. Accordingly, we set out to characterize the pharmacokinetic properties of glioma-tropic oncolytic adenovirus loaded HB1.F3-CD carrier system in three different animal models: nude mouse, hamster and cotton rat. We show that NSCs can be loaded with CRAd-S-pk7 and release new infectious progeny that can effectively lyse glioma cells. We observed that when injected in mice brains bearing human glioma xenograft, NSCs loaded with CRAd-S-pk7 home to glioma and hand off therapeutic adenoviral payload to tumor cells. In models permissive to adenovirus

replication, hamster and cotton rat, we detect high adenoviral E1A replication only at the injection site. Furthermore, adenoviral replication declines and becomes barely detectable over 30 days. On the other hand, we detect implanted NSCs only at the injected hemisphere for less than a week. Thus, data presented in this report argue in favor of the possible future utilization of a neural stem cell-based carrier to enhance the therapeutic potential of the anti-glioma oncolytic virotherapy.

The clinical outcome of any cell carrier system for oncolytic virotherapy relies on proper synchronization of three critical steps in both space and time[25]. The ideal carrier cell should i) be easily infected with the therapeutic virus; ii) produce high levels of progeny that can infect target tumor cells; iii) be relatively resistant to oncolytic virus-mediated toxicity. Even though the HB1.F3-CD cell carrier system express a very minimal amount of the primary adenovirus attachment receptors (CAR) (Figure 1a), they express high levels (50%) of CD138 (Syndecan), a heparan sulfate proteoglycan receptor that binds to the polylysine residues (pk7) of modified CRAd-S-pk7 fibers. The adenoviral internalization into target cells is mediated by the integrin family receptors αvβ3 and αvβ5 and almost 91.2% of HB1.F3-CD cells express αvβ5 on their surface. Once internalized, the virus starts replicating its genome within 24 hours and gradually increases over time (Figure 1d, 2a). The cell associated infectious progeny reached its maximum at day 5-post infection, while the cell free virus titer reached its peak at 1×10^9 i.u./ml after 7 days of infection (Figure 2a). The fundamental objective of the *ex vivo* loading phase is to productively load/infect as many cell carriers as possible with minimal exposure to the therapeutic virus. With the loading dose of 50 i.u./cell, we observed the maximum amount of viral DNA replication and only about a 25% decrease in the carrier cell viability at 120 hours post loading (Figure 1b, c). Based on this data we selected a loading dose of 50 i.u./cell to use in all our future experiments. For our system, the infection of HB1.F3-CD cells in suspension with the CRAd-S-pk7 at a loading dose of 50 i.u./cell lead to the infection of almost 100% of carrier cells after a period of 2 hours (Figure 1e, 1f). It is probably necessary to optimize the *ex vivo* loading capacity of each carrier cell/oncolytic virus pair system as it's governed by the oncolytic virus life cycle within the particular cell type used for delivery; for example the standard infection protocol for VSV infection specify a shorter (1hour) loading time for Vaccinia virus[25].

An effective cell carrier system must be able to produce high quantities of infectious progeny upon arrival at the tumor site. HB1.F3-CD cells loaded/infected with 1 i.u./cell of CRAd-S-pk7 virus produced sufficient amounts of infectious progeny to induce oncolysis on human glioma cell lines (Figure 2b, c). Moreover, loaded cells produced high intratumoral levels of progeny at the tumor site that were similar to naked CRAd injection (Figure 6c, d). Most importantly intracranial delivery of the oncolytic adenovirus loaded into HB1.F3-CD significantly decreased the unwanted distribution of therapeutic virus out of the animal brain (***$p<0.001$), thus reducing the vector related toxicity (Figure 7a). Our lab has previously shown that cell carriers can deliver CRAd-S-pk7 to the tumor site when injected at a distance from the tumor[15, 16]. We have further shown that NSCs tumor tropic properties are not diminished by the loading/infection of oncolytic adenovirus[17].

The timing of the oncolytic viral life cycle is a crucial determinant of maintaining the tumor homing ability of the carrier cells. To achieve true 'targeted-delivery' of the therapeutic virus, the carrier cell must accumulate in tumor beds before the viral progeny are released. According to our *in vitro* observation, the viral progeny released from the HB1.F3-CD carrier cell peaked at day 7 post loading (Figure 2a), therefore carrier cells should ideally reach the tumor site before this time. Based on our previous study, a majority of the tumor specific migration of NSCs occurred within 24–48 hours post implantation[17]. Therefore, the replication cycle of CRAd-S-pk7 oncolytic virus in the HB1.F3-CD should accommodate the tumor homing ability of this carrier system.

The preclinical characterization of most oncolytic adenovirus vectors have thus far been restricted to human xenograft models in immunodeficient mice. While these immunodeficient mice can serve as valuable models to evaluate the therapeutic efficacy of adenovirus based oncolytic vectors, the virus does not replicate in mouse tissue, and therefore prevents us from being able to vigorously evaluate safety and vector related toxicity. On the other hand, semi-permissive animal models to adenovirus replication, such as cotton rat and hamster, have proven to be very useful for studying oncolytic adenovirus safety profiles[26–28]. Accordingly, we characterized the CRAd-S-pk7 biodistribution and safety profile after intracranial delivery of loaded NSCs in these immunocompetent animal models. To assess the distribution of both the adenovirus and carrier cell we relied on very sensitive PCR methods (Supplementary Figure S1, S2). Both models show similar distribution of NSCs and CRAd-S-pk7. NSCs are found only at the injection site without any non-specific migration. However, we observed a decreased amount of the non-specific spread of CRAd when delivered with the carrier cell system, as evidenced by the 2 log lower adenoviral titers in the contralateral hemisphere (Figure 6b, 6c and 7a). It has been previously reported that after intracranial delivery the oncolytic virus can spread throughout the brain due to the presence of media such as cerebro-spinal fluid (CSF)[29]. However, this may be less of a concern as compared to other target tissue, such as the liver, as the effect of neutralizing antibody appears to be far weaker in the brain due to the distinct nature of the immune system in the CNS[30, 31]. Moreover, reports from early clinical trials with adenovirus vector-based anti-glioma gene therapy have uniformly reported sufficient tolerability and absence of serious adverse events[32]. In our study, after the delivery via carrier cells, adenovirus replication in the brain decreased to barely detectable levels over 30 days. Also, very low levels of adenovirus E1A copies were detected in the other harvested organs (Figure 7a) and none of the animals implanted with NSC loaded CRAd-S-pk7 showed any sign of systemic toxicity. Taken together, we conclude the intracranial injection of adenovirus loaded NSCs appears safe in all three tested animal models with no adverse side effects observed. In our experience, even though cotton rats were able to support oncolytic adenovirus replication more effectively than hamsters[21], they are more aggressive and difficult to handle during any surgical procedure[33, 34].

Most of the pre-clinical studies on the efficacy of NSC-based anti-glioma therapeutics have been evaluated to target disseminated tumor sites beyond the primary tumor in small animal models. But can NSCs withstand the test of distance and deliver to metastatic sites far away from the site of injection in a human brain? The failures of gene therapy can be undoubtedly

linked to inaccessibility of optimal animal models that recapitulate human GBM and therefore we should be cautious when attempting to translate our findings into clinical trials. For example, it becomes imperative to study the efficacy of virus loaded cell carriers in animals with larger brains and therefore larger sized tumors than nude mice. As one of the possible options, a spontaneous GBM model in the brachycephalic canine breeds has been reported[35]. Canine GBM is highly invasive and mimics human GBM characteristics such as necrosis with pseudopalisading, neovascularization, and endothelial proliferation[36]. The most important aspect of the canine model is its comparable brain size to humans. This characteristic is essential for a good preclinical model in order to precisely assess such pharmacokinetic properties as toxicity, dosage, side effects, as well as more accurately measure delivery strategies.

Furthermore, the therapeutic efficacy of most anti-glioma gene therapeutic approaches are commonly evaluated in immunocompromised animal models using xenogenic cell lines post transplantation with only a short interval of time between engraftment and treatment. The circumstances in human GBM completely differ as tumor initiation is usually sporadic and clinical symptoms can be observed months to years after initial establishment of tumor, resulting in increased heterogeneity. Moreover, when a carrier cell system is injected into animal models such as the one used in our study, it becomes vulnerable to the immune response generated towards any foreign antigen. We observed the effects of such an immune response when we noticed a rapid decline of implanted stem cell numbers in the immunocompetent cotton rat and hamster models over time (Figure 7b–d). As a result, the NSC viability is even more affected in immunocompetent animal models as compared to immunocompromised nude mice (Figures 3 and 4). In the clinical setting, we do expect to encounter some degree of immune response towards the stem cell-based carrier as the immortalized HB1.F3.CD cell line will be mismatched to human leukocyte antigens and thus will be allogeneic to glioma patients. Despite low expression of MHC class II and co-stimulatory molecules, in vitro allorecognition of NSCs by peripheral blood lymphocytes has been reported[37, 38]. These observations do argue in favor of the use of readily available autologous NSC sources. However, there are some serious limitations to currently available technologies for isolating and expanding autologous NSCs in culture in order to produce a sufficient number of viable cells for a successful transplantation. If grafting of the carrier cell becomes an issue in the clinical setting, we may have to consider utilization of immunosuppressive drugs in order to prolong the half-life of the therapeutic NSCs.

Although, the HB1.F3-CD cell line per se has been approved by the FDA for clinical trials in recurrent glioma (NCT01172964), nevertheless the human immune system may impact the viability of adenovirus loaded cells since patients will have antibodies towards adenoviral antigens. Taking this into consideration, our study has led us to expect such an immune response to be less robust as compared to direct adenovirus injection[18]. Most currently available cancer gene therapies have failed to sustain anti-tumor effects in the tumor microenvironment long enough to achieve clinically relevant therapeutic efficacy[39]. This is partly due to the mounting of a host immune response against the administered therapeutic agents. A wealth of preclinical data suggests that *in vivo* transplanted NSCs can act as immunosuppressants[40]. Results from several studies in both rodent and non-human

primate models of experimental autoimmune encephalomyelitis (EAE) indicate that NSCs transplanted by either intrathecal or intravenous injection promote bystander immunodulation within the CNS via the release of various soluble molecules[40, 41]. We reported that CRAd loaded NSC transiently secret immunosupressive cytokines IL-10 and significantly reduced CRAd mediated CNS injury[17]. This immunosuppressive quality of NSCs is a very attractive attribute for a cell carrier given that it will allow therapeutic payloads such as oncolytic viruses to be shielded from host immunosurveillance. Therefore, we propose that our delivery system would prove safer than the direct virus injection into the tumor.

In summary, we have demonstrated that a neural stem cell-based cell carrier can significantly improve the safety and biodistribution profile of the anti-glioma oncolytic virotherapy in an animal model. Such a carrier system has shown the ability to support the delivery of a similar dose of therapeutic virus at the implanted site, as compared to a naked virus, and also reduce the leaky distribution of the virus throughout the animal brain. Moreover, we compare nude mouse, cotton rat and hamster animal models to evaluate the pharmacological and safety profiles of the cell-based oncolytic virotherapy. This information will be useful to other investigators who are interested in utilizing the cell carrier approach to achieve targeted delivery of oncolytic virus to metastatic tumor burdens in cancer patients and translating cell carrier-based oncolytic virotherapy to the clinic.

Supplementary Material

Refer to Web version on PubMed Central for supplementary material.

Acknowledgements

We would like to thank Simona M. Ahmed and Brenda Auffinger for editing the manuscript; Feifei Liu and Lingjiao Zhang for statistical analysis. This research was supported by the NCI (R01CA122930, R01CA138587), the National Institute of Neurological Disorders and Stroke (U01NS069997), and the American Cancer Society (RSG-07-276-01-MGO).

References

1. Deorah S, Lynch CF, Sibenaller ZA, Ryken TC. Trends in brain cancer incidence and survival in the United States: Surveillance, Epidemiology, and End Results Program, 1973 to 2001. Neurosurg Focus. 2006; 20(4):E1. [PubMed: 16709014]
2. Stupp R, Hegi ME, Mason WP, van den Bent MJ, Taphoorn MJ, Janzer RC, et al. Effects of radiotherapy with concomitant and adjuvant temozolomide versus radiotherapy alone on survival in glioblastoma in a randomised phase III study: 5-year analysis of the EORTC-NCIC trial. Lancet Oncol. 2009; 10(5):459–466. [PubMed: 19269895]
3. Wen PY, Kesari S. Malignant gliomas in adults. N Engl J Med. 2008; 359(5):492–507. [PubMed: 18669428]
4. Sheehan JP, Shaffrey ME, Gupta B, Larner J, Rich JN, Park DM. Improving the radiosensitivity of radioresistant and hypoxic glioblastoma. Future Oncol. 2010; 6(10):1591–1601. [PubMed: 21062158]
5. Sampson JH, Heimberger AB, Archer GE, Aldape KD, Friedman AH, Friedman HS, et al. Immunologic escape after prolonged progression-free survival with epidermal growth factor receptor variant III peptide vaccination in patients with newly diagnosed glioblastoma. J Clin Oncol. 2010; 28(31):4722–4729. [PubMed: 20921459]

6. Bao S, Wu Q, Sathornsumetee S, Hao Y, Li Z, Hjelmeland AB, et al. Stem cell-like glioma cells promote tumor angiogenesis through vascular endothelial growth factor. Cancer Res. 2006; 66(16): 7843–7848. [PubMed: 16912155]
7. Dey M, Ulasov IV, Tyler MA, Sonabend AM, Lesniak MS. Cancer Stem Cells: The Final Frontier for Glioma Virotherapy. Stem Cell Rev. 2011; 7(1):119–129. [PubMed: 20237963]
8. Kelly E, Russell SJ. History of oncolytic viruses: genesis to genetic engineering. Mol Ther. 2007; 15(4):651–659. [PubMed: 17299401]
9. Ulasov IV, Zhu ZB, Tyler MA, Han Y, Rivera AA, Khramtsov A, et al. Survivin-driven and fiber-modified oncolytic adenovirus exhibits potent antitumor activity in established intracranial glioma. Hum Gene Ther. 2007; 18(7):589–602. [PubMed: 17630837]
10. Zhu ZB, Makhija SK, Lu B, Wang M, Rivera AA, Kim-Park S, et al. Incorporating the survivin promoter in an infectivity enhanced CRAd-analysis of oncolysis and anti-tumor effects in vitro and in vivo. Int J Oncol. 2005; 27(1):237–246. [PubMed: 15942665]
11. Ulasov IV, Rivera AA, Sonabend AM, Rivera LB, Wang M, Zhu ZB, et al. Comparative evaluation of survivin, midkine and CXCR4 promoters for transcriptional targeting of glioma gene therapy. Cancer Biol Ther. 2007; 6(5):679–685. [PubMed: 17404502]
12. Jiang H, Gomez-Manzano C, Aoki H, Alonso MM, Kondo S, McCormick F, et al. Examination of the therapeutic potential of Delta-24-RGD in brain tumor stem cells: role of autophagic cell death. J Natl Cancer Inst. 2007; 99(18):1410–1414. [PubMed: 17848677]
13. Selznick LA, Shamji MF, Fecci P, Gromeier M, Friedman AH, Sampson J. Molecular strategies for the treatment of malignant glioma--genes, viruses, and vaccines. Neurosurg Rev. 2008; 31(2): 141–155. discussion 155. [PubMed: 18259789]
14. Chiocca EA, Aguilar LK, Bell SD, Kaur B, Hardcastle J, Cavaliere R, et al. Phase IB Study of Gene-Mediated Cytotoxic Immunotherapy Adjuvant to Up-Front Surgery and Intensive Timing Radiation for Malignant Glioma. J Clin Oncol. 2011; 29(27):3611–3619. [PubMed: 21844505]
15. Tyler MA, Ulasov IV, Sonabend AM, Nandi S, Han Y, Marler S, et al. Neural stem cells target intracranial glioma to deliver an oncolytic adenovirus in vivo. Gene Ther. 2009; 16(2):262–278. [PubMed: 19078993]
16. Sonabend AM, Ulasov IV, Tyler MA, Rivera AA, Mathis JM, Lesniak MS. Mesenchymal stem cells effectively deliver an oncolytic adenovirus to intracranial glioma. Stem Cells. 2008; 26(3): 831–841. [PubMed: 18192232]
17. Ahmed AU, Thaci B, Alexiades NG, Han Y, Qian S, Liu F, et al. Neural Stem Cell-based Cell Carriers Enhance Therapeutic Efficacy of an Oncolytic Adenovirus in an Orthotopic Mouse Model of Human Glioblastoma. Mol Ther. 2011; 19(9):1714–1726. [PubMed: 21629227]
18. Ahmed AU, Tyler MA, Thaci B, Alexiades NG, Han Y, Ulasov IV, et al. A comparative study of neural and mesenchymal stem cell-based carriers for oncolytic adenovirus in a model of malignant glioma. Mol Pharm. 2011; 8(5):1559–1572. [PubMed: 21718006]
19. Dembinski JL, Spaeth EL, Fueyo J, Gomez-Manzano C, Studeny M, Andreeff M, et al. Reduction of nontarget infection and systemic toxicity by targeted delivery of conditionally replicating viruses transported in mesenchymal stem cells. Cancer Gene Ther. 2010; 17(4):289–297. [PubMed: 19876078]
20. Kim SK, Kim SU, Park IH, Bang JH, Aboody KS, Wang KC, et al. Human neural stem cells target experimental intracranial medulloblastoma and deliver a therapeutic gene leading to tumor regression. Clin Cancer Res. 2006; 12(18):5550–5556. [PubMed: 17000692]
21. Sonabend AM, Ulasov IV, Han Y, Rolle CE, Nandi S, Cao D, et al. Biodistribution of an oncolytic adenovirus after intracranial injection in permissive animals: a comparative study of Syrian hamsters and cotton rats. Cancer Gene Ther. 2009; 16(4):362–372. [PubMed: 19011597]
22. Aboody KS, Najbauer J, Danks MK. Stem and progenitor cell-mediated tumor selective gene therapy. Gene Ther. 2008; 15(10):739–752. [PubMed: 18369324]
23. Thu MS, Najbauer J, Kendall SE, Harutyunyan I, Sangalang N, Gutova M, et al. Iron labeling and pre-clinical MRI visualization of therapeutic human neural stem cells in a murine glioma model. PLoS One. 2009; 4(9):e7218. [PubMed: 19787043]

24. Ahmed AU, Rolle CE, Tyler MA, Han Y, Sengupta S, Wainwright DA, et al. Bone marrow mesenchymal stem cells loaded with an oncolytic adenovirus suppress the anti-adenoviral immune response in the cotton rat model. Mol Ther. 2010; 18(10):1846–1856. [PubMed: 20588259]
25. Power AT, Bell JC. Taming the Trojan horse: optimizing dynamic carrier cell/oncolytic virus systems for cancer biotherapy. Gene Ther. 2008; 15(10):772–779. [PubMed: 18369325]
26. Toth K, Spencer JF, Tollefson AE, Kuppuswamy M, Doronin K, Lichtenstein DL, et al. Cotton rat tumor model for the evaluation of oncolytic adenoviruses. Hum Gene Ther. 2005; 16(1):139–146. [PubMed: 15703497]
27. Toth K, Spencer JF, Wold WS. Immunocompetent, semi-permissive cotton rat tumor model for the evaluation of oncolytic adenoviruses. Methods Mol Med. 2007; 130:157–168. [PubMed: 17401171]
28. Thomas MA, Spencer JF, Wold WS. Use of the Syrian hamster as an animal model for oncolytic adenovirus vectors. Methods Mol Med. 2007; 130:169–183. [PubMed: 17401172]
29. Studebaker AW, Hutzen B, Pierson CR, Russell SJ, Galanis E, Raffel C. Oncolytic measles virus prolongs survival in a murine model of cerebral spinal fluid-disseminated medulloblastoma. Neuro Oncol. 2012
30. Lowenstein PR. Immunology of viral-vector-mediated gene transfer into the brain: an evolutionary and developmental perspective. Trends Immunol. 2002; 23(1):23–30. [PubMed: 11801451]
31. Bessis N, GarciaCozar FJ, Boissier MC. Immune responses to gene therapy vectors: influence on vector function and effector mechanisms. Gene Ther. 2004; 11(Suppl 1):S10–S17. [PubMed: 15454952]
32. Pulkkanen KJ, Yla-Herttuala S. Gene therapy for malignant glioma: current clinical status. Mol Ther. 2005; 12(4):585–598. [PubMed: 16095972]
33. Niewiesk S, Prince G. Diversifying animal models: the use of hispid cotton rats (Sigmodon hispidus) in infectious diseases. Lab Anim. 2002; 36(4):357–372. [PubMed: 12396279]
34. Niewiesk S. Cotton rats (Sigmodon hispidus): an animal model to study the pathogenesis of measles virus infection. Immunol Lett. 1999; 65(1–2):47–50. [PubMed: 10065626]
35. Candolfi M, Curtin JF, Nichols WS, Muhammad AG, King GD, Pluhar GE, et al. Intracranial glioblastoma models in preclinical neuro-oncology: neuropathological characterization and tumor progression. J Neurooncol. 2007; 85(2):133–148. [PubMed: 17874037]
36. Stoica G, Lungu G, Martini-Stoica H, Waghela S, Levine J, Smith R 3rd. Identification of cancer stem cells in dog glioblastoma. Vet Pathol. 2009; 46(3):391–406. [PubMed: 19176492]
37. Ubiali F, Nava S, Nessi V, Frigerio S, Parati E, Bernasconi P, et al. Allorecognition of human neural stem cells by peripheral blood lymphocytes despite low expression of MHC molecules: role of TGF-beta in modulating proliferation. Int Immunol. 2007; 19(9):1063–1074. [PubMed: 17660500]
38. Ahmed AU, Alexiades NG, Lesniak MS. The use of neural stem cells in cancer gene therapy: predicting the path to the clinic. Curr Opin Mol Ther. 2010; 12(5):546–552. [PubMed: 20886386]
39. Cattaneo R, Miest T, Shashkova EV, Barry MA. Reprogrammed viruses as cancer therapeutics: targeted, armed and shielded. Nat Rev Microbiol. 2008; 6(7):529–540. [PubMed: 18552863]
40. Einstein O, Ben-Hur T. The changing face of neural stem cell therapy in neurologic diseases. Arch Neurol. 2008; 65(4):452–456. [PubMed: 18413466]
41. Pluchino S, Quattrini A, Brambilla E, Gritti A, Salani G, Dina G, et al. Injection of adult neurospheres induces recovery in a chronic model of multiple sclerosis. Nature. 2003; 422(6933): 688–694. [PubMed: 12700753]

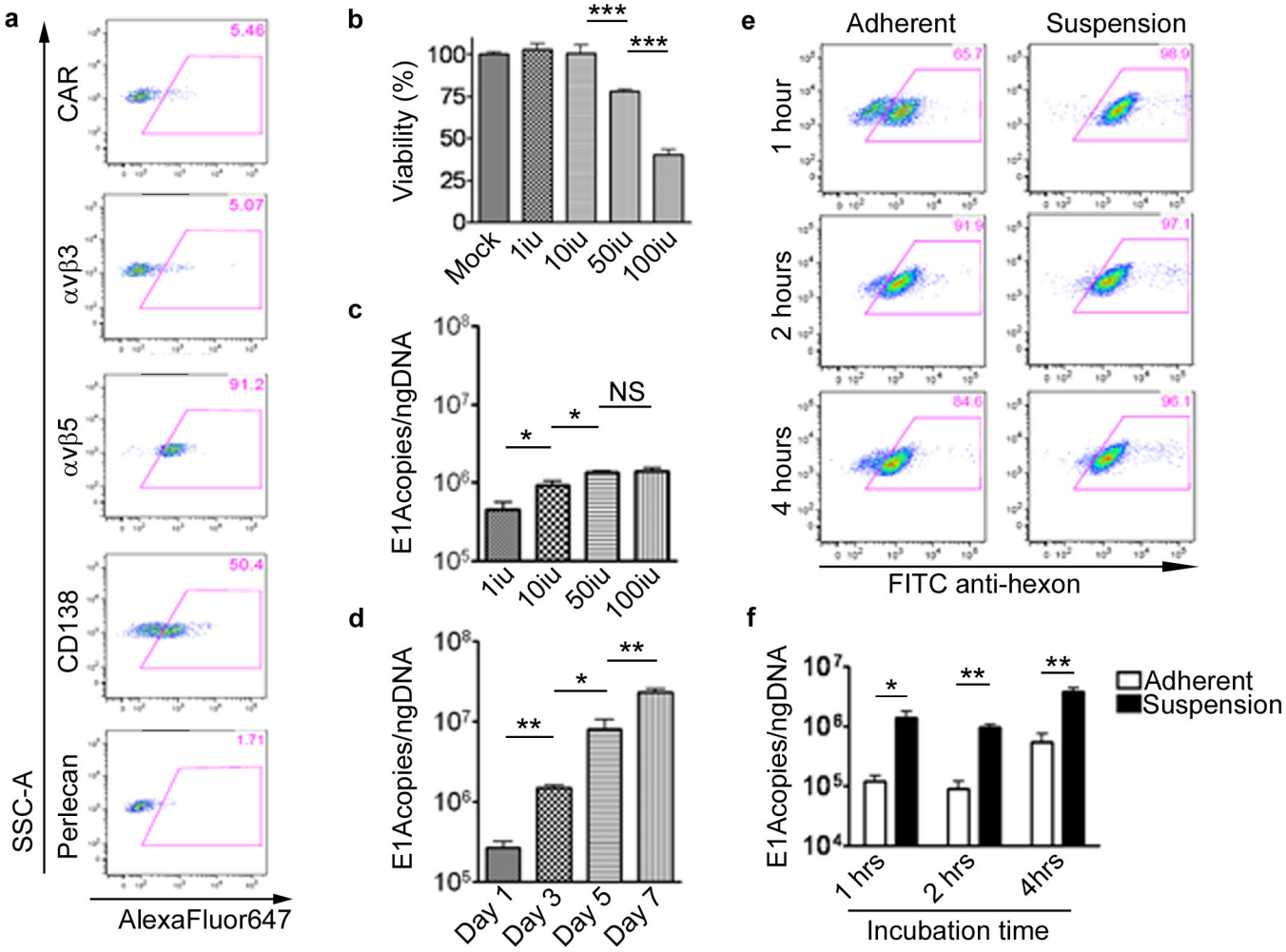

Figure 1.

HB1.F3-CD neural stem cell line is permissive to CRAd-S-pk7 replication. (**a**) HB1.F3-CD cells were stained for surface antigens, known to participate in adenovirus anchorage. Numbers in the top right corner of each dot plot represent percentages of positive cells. Gates were drawn based on an isotype control stained sample. y-Axis, SSC-A; x-axis, AlexaFluor647-A. (**b**) Cytopathic effects of CRAd-S-pk7 on HB1.F3-CD cells. Cells were infected with different concentrations of CRAd-S-pk7 (1, 10, 50 and 100i.u.) and viability was evaluated by MTT viability assay at day 5 post-infection. (**c–d**) The replicative capacity of CRAd-S-pk7 was measured by quantitative RT-PCR and presented as number of viral E1A copies per ng of DNA from the infected cells. The extent of viral replication was determined at day 3 post-infection (**c**) with different concentrations of CRAd-S-pk7 and at the indicated time points after infection (**d**) with 50 i.u. of CRAd-S-pk7. To determine the best loading conditions for NSCs we infected the carrier cells in adherent vs. suspension conditions at different time intervals. Transduction efficiency was determined via flow cytometry (**e**) for adenovirus hexon protein. Instead, the adenovirus replication was quantified via quantitative RT-PCR (**f**). All conditions were conducted in triplicates and

repeated in three separate experiments (error bars represent standard error of measurement (SEM); ***, P-value <0.001; **, P-value <0.01; *, P-value <0.05; NS, not significant).

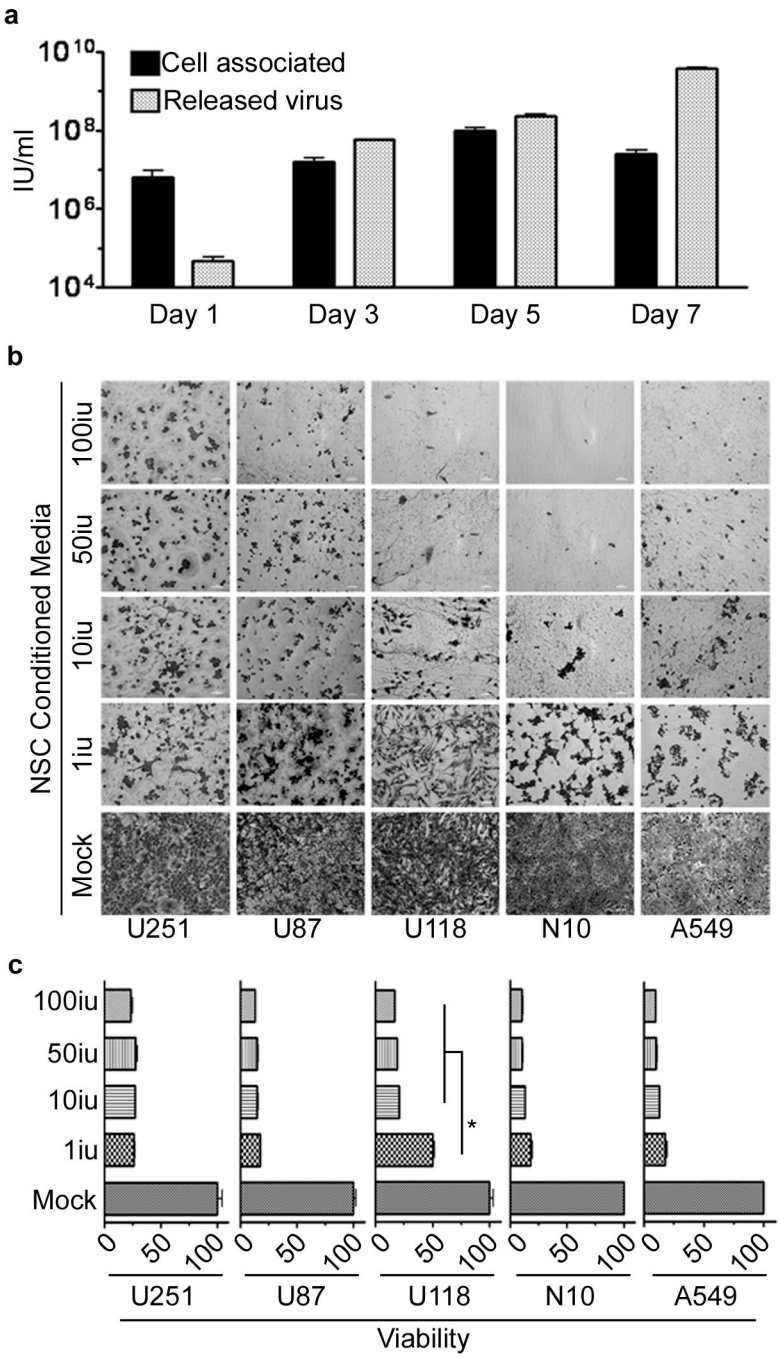

Figure 2.

Adenoviral progeny released from infected HB1.F3-CD effectively lyses glioma cell lines. (**a**) The supernatant and cells, infected with 50 i.u./cell of CRAd-S-pk7, were collected and analyzed separately. The viral progeny inside the cells (cell associated) and the progeny released by the infected cells (released virus) over time were measured by the titer assay. The supernatant of HB1.F3-CD cells infected with different concentrations of CRAd-S-pk7 (0, 1, 10, 50 and 100 i.u./cell) was collected 5 days post-infection and used to infect different glioma cell lines (U87, U251, U118 and N10) and a lung adenocarcinoma cell line (A549).

Viability was assessed 3 days later via crystal violet staining (**b**) and MTT viability assay (**c**). Error bars represent SEM; *, P-value <0.05.

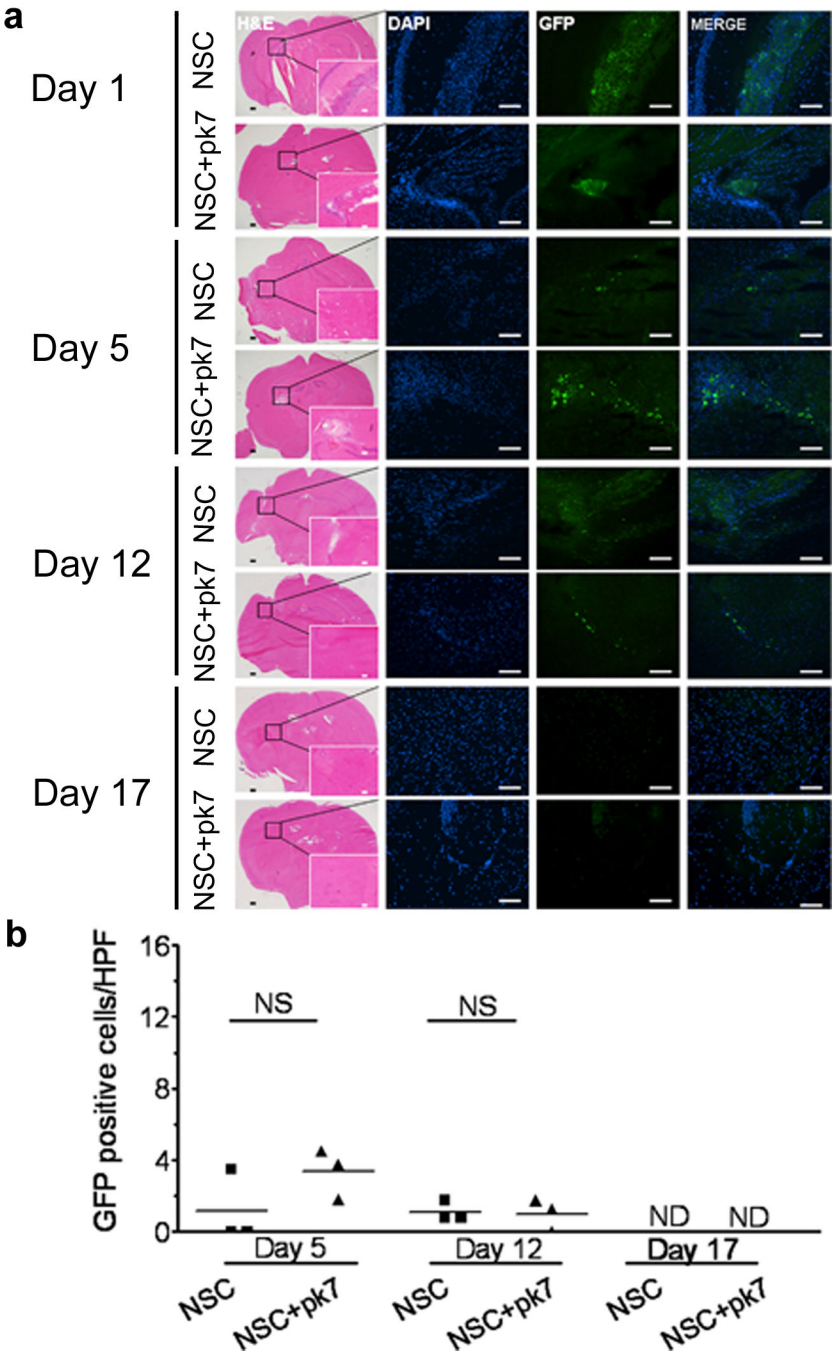

Figure 3.

Intracranial distribution of the HB1.F3-CD carrier cells loaded or not with CRAd-S-pk7 after injection in nude mouse brains. (**a**) 9–10 week old nude mice were injected in the right hemisphere, 3 mm deep, with 5×10^5 HB1.F3-CD-GFP cells loaded or not with 50 i.u. of CRAd-S-pk7. Intracranial distribution of GFP positive cells was evaluated at the indicated time points for both loaded and non-loaded cells (n=3 per time point per group). (**b**) Positive GFP cells were quantified based on number of cells per high power field (HPF) (630×).

Values on the y axis represent the mean number of GFP positive cells per HPF for each animal. *Bars: 400μm (H&E); 100μm (IHC). NS, not significant; ND, none detected.*

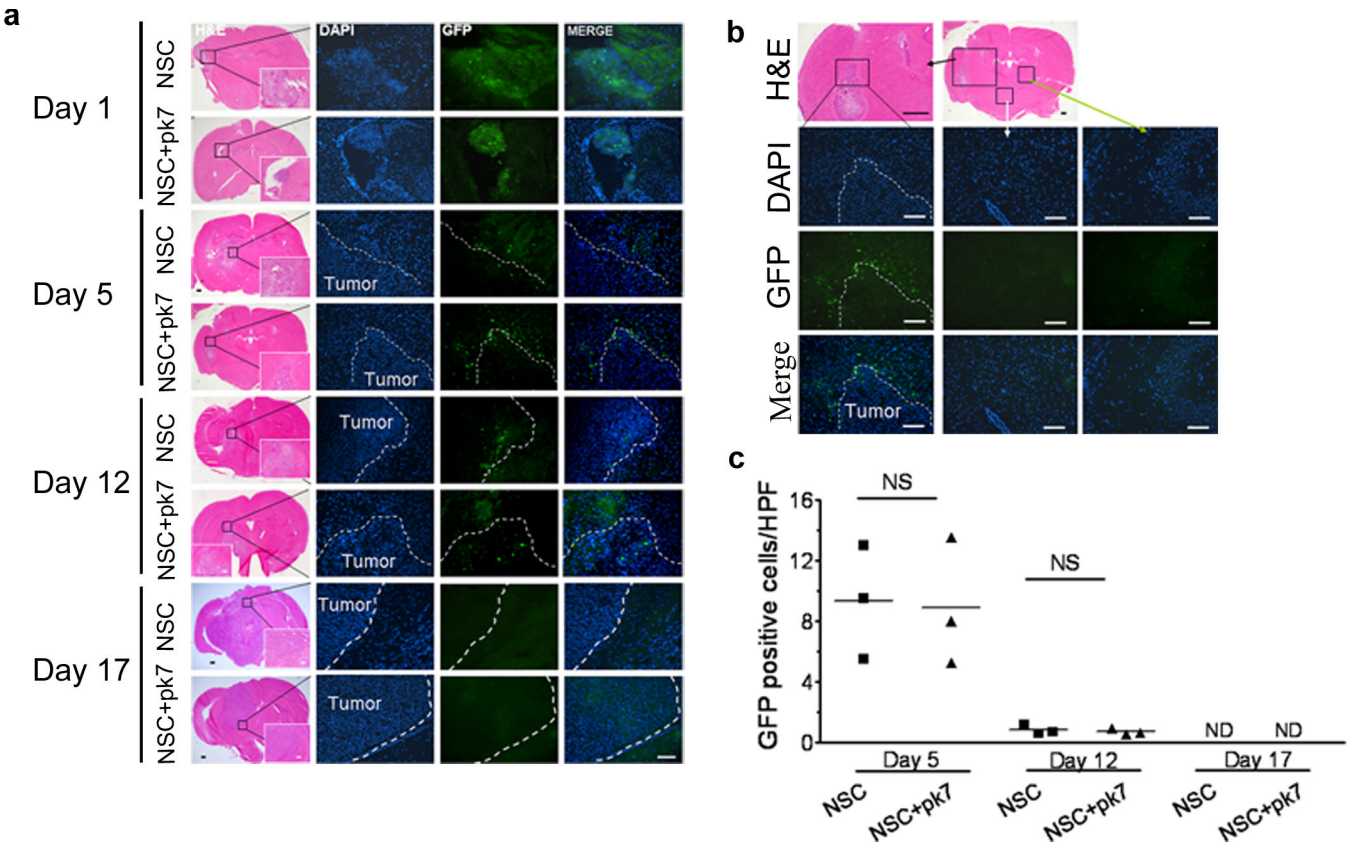

Figure 4.

Intracranial distribution of the HB1.F3-CD carrier cells loaded or not with CRAd-S-pk7 after injection in nude mouse brains bearing human orthotopic U87 glioma xenografts. (**a**) 7 week old nude mice were injected in the right hemisphere, 3 mm deep, with 2×10^5 U87 malignant glioma cells. Three weeks later, 5×10^5 HB1.F3-CD-GFP cells loaded or not with 50 i.u CRAd-S-pk7 were injected in the right hemisphere using the same burr-hole. Intracranial distribution of GFP positive cells was evaluated at the indicated time points for both loaded and non-loaded cells (n=3 per time point per group). (**b**) A representative distribution of the carrier cells at day 5 post-injection. GFP positive cells are found at the glioma-brain interface (depicted in the left column); while no GFP cells were detected elsewhere in the brain (the middle and right column). (**c**) Positive GFP cells in the glioma-brain interface were quantified based on number of cells per high power field (HPF) (630×). Values in y axis represent the mean number of GFP positive cells per HPF for each animal. *Bars: 400μm (H&E); 100μm (IHC). NS, not significant; ND, none detected.*

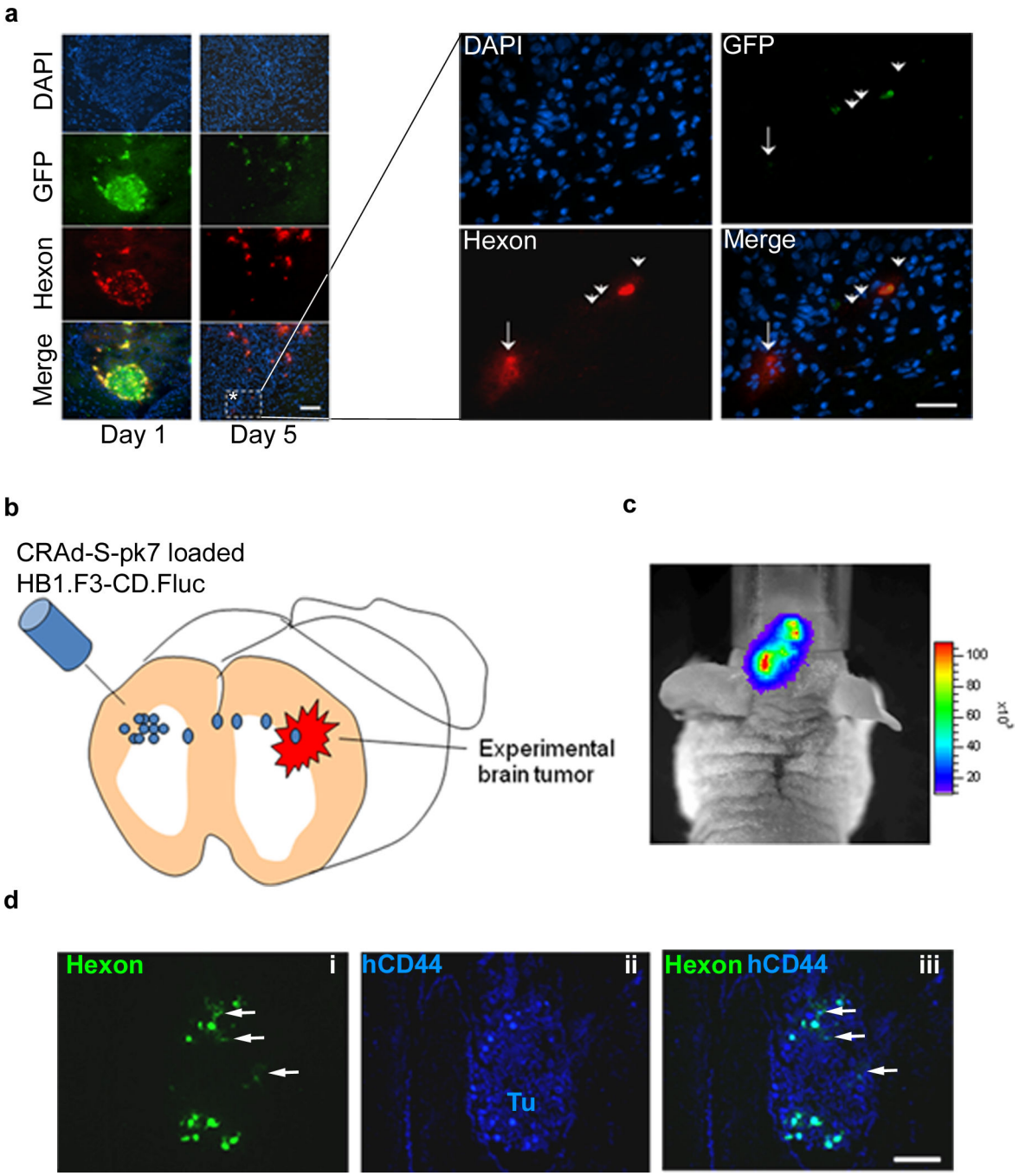

Figure 5.

In vivo hand-off of CRAd-S-pk7 from NSCs to glioma cells. (**a**) Nude mice harboring orthotopic U87 malignant glioma in the right hemisphere were injected with HB1.F3-CD-GFP cells loaded or not with CRAd-S-pk7, using the same burr-hole. *In vivo* CRAd-S-pk7 hand-out from infected GFP-labeled HB1.F3-CD to U87 glioma cells was detected via immunohistochemistry. A representative area within the tumor where hand out of CRAd-S-pk7 is evident (*) was magnified and shown in the right panel. Cells that are positive for both GFP and hexon (arrowheads) represent infected HB1.F3-CD that are releasing

adenovirus; while hexon-positive, GFP-negative, DAPI positive (arrow) represent glioma cells infected with adenovirus. To show that loaded NSCs can travel longer distances and still successfully deliver adenovirus, we injected CRAd-S-pk7 loaded HB1.F3-CD.Fluc in the contralateral hemisphere **(b)**. Migration of NSCs was visualized via photonflux imaging at 72 hour **(c)**. **(d)** To show that migrating NSCs were still replicating and releasing adenovirus animals were sacrificed at 72 hours post NSC injection; we stained tumor containing sections with antibodies for adenovirus hexon (i) and human CD44 (ii) to evidentiate human glioma cells. Tu, tumor *Bars: 100μm.*

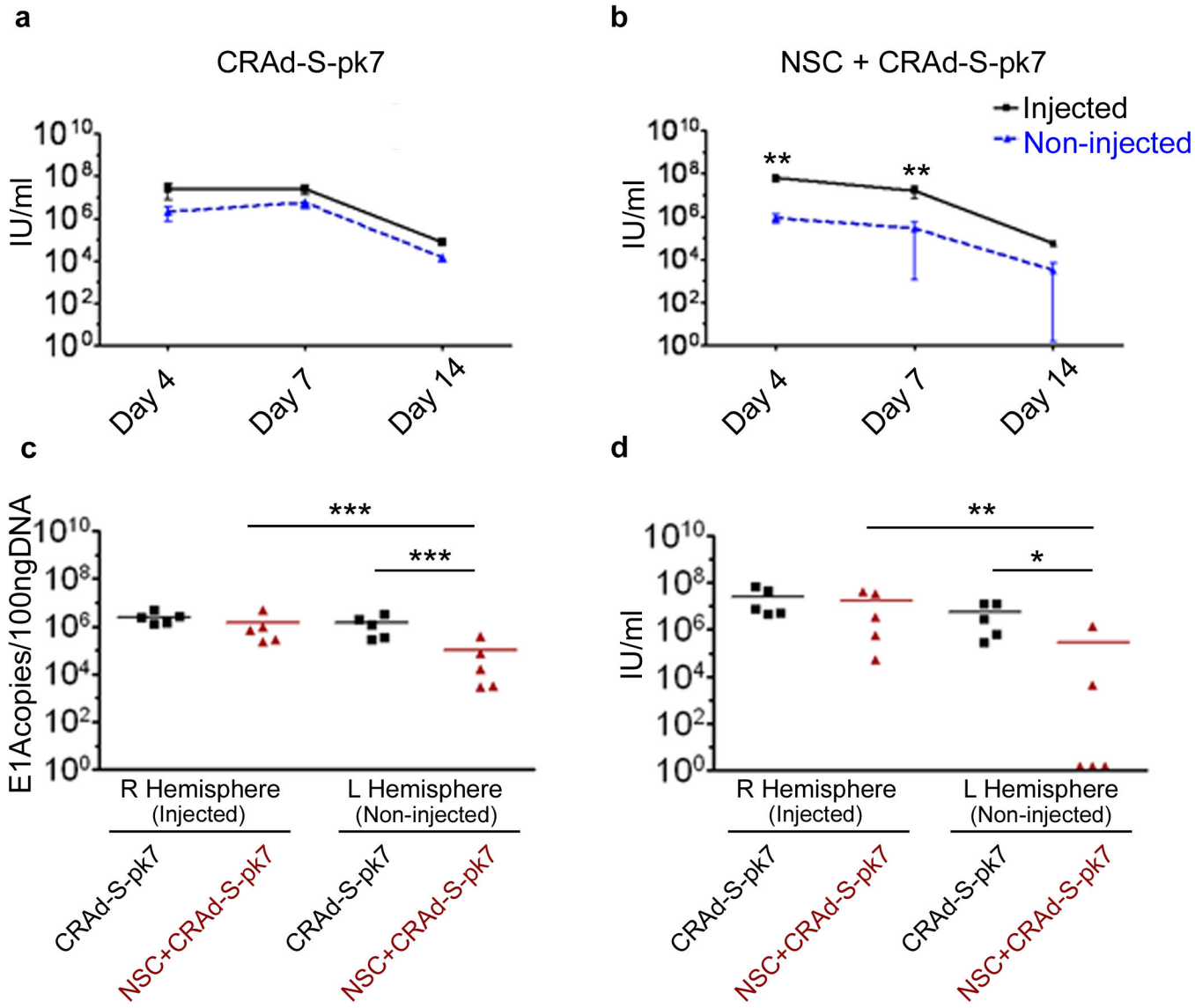

Figure 6.

Carrier cell adenovirus delivery achieves lower off-site viral titers. Nude mice harboring orthotopic U87 malignant glioma in the right hemisphere were injected, using the same burr-hole, with HB1.F3-CD-GFP cells loaded with CRAd-S-pk7 or the equivalent amount of oncolytic adenovirus (2.5×10^7 i.u./mouse). *In vivo* CRAd-S-pk7 replication (n=5 per group per time point) was quantified for each hemisphere separately (right hemisphere/injected vs. left hemispheres/non-injected) via qRT-PCR **(a, b)** for adenoviral E1A and by adenoviral progeny titer assay **(c, d)**. *Error bars represent SEM; ***, P-value <0.001; **, P-value <0.01; *, P-value <0.05; Non significant differences are not depicted.*

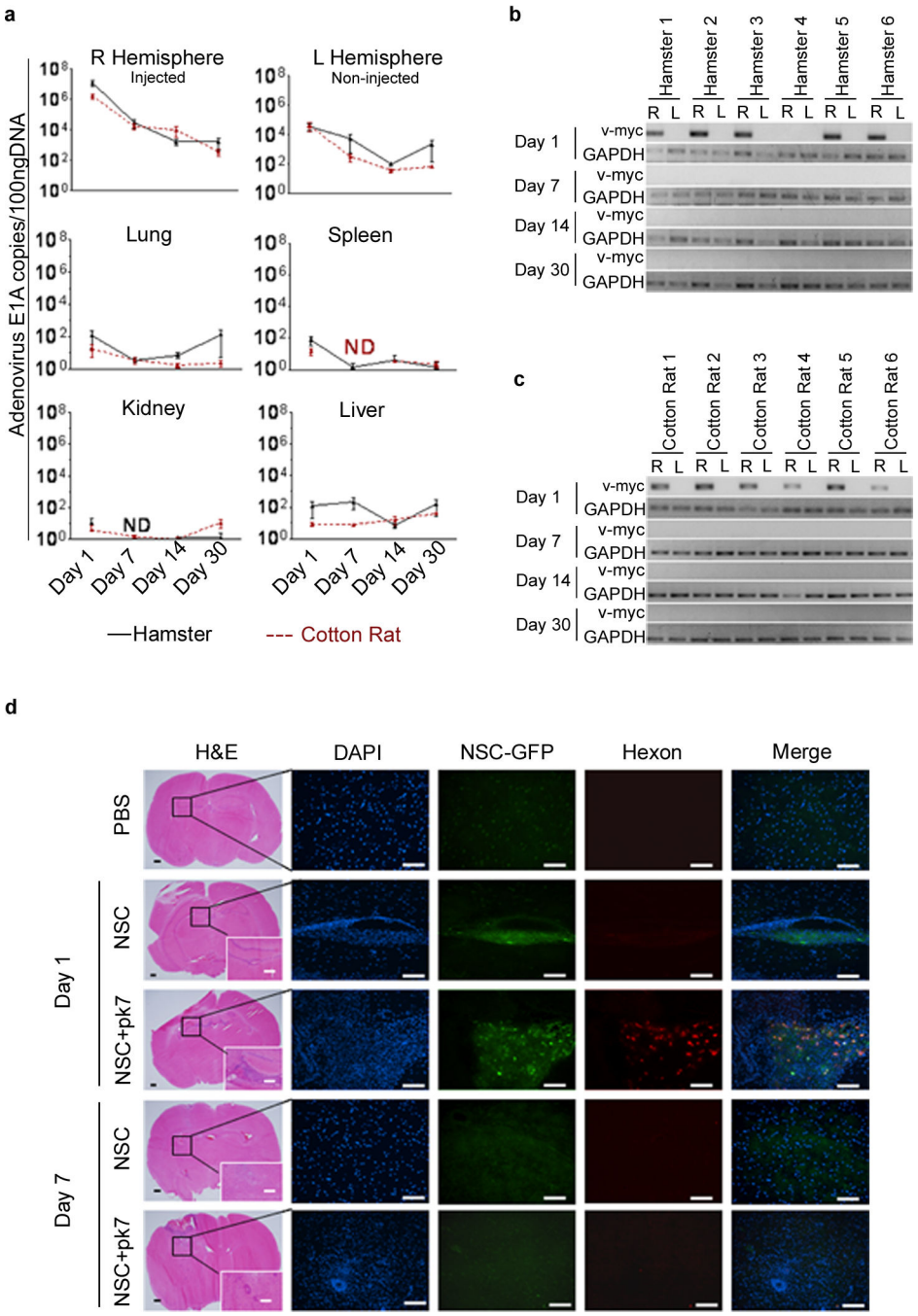

Figure 7.

Biodistribution of CRAd-S-pk7 and HB1.F3-CD in hamsters and cotton rats. (**a**) Animals were injected intracranially (right hemisphere) with HB1.F3-CD cells loaded with CRAd-S-pk7 and sacrificed at the indicated time points (n=6 per time point). Brains and other organs were harvested and adenovirus biodistribution was evaluated using qRT-PCR for E1A. HB1.F3-CD intracranial distribution in hamster **(b)** and cotton rat **(c)** was evaluated by using a highly sensitive two-step nested PCR for *v-myc*. Presence of NSCs in each hemisphere was analyzed separately: right (R) vs. left (L). For DNA loading control, in the nested PCR, we

used a housekeeping gene (GAPDH). (**d**) Intracranial distribution of the HB1.F3-CD carrier cells loaded or not with CRAd-S-pk7 after injection in hamster brains. Animals were injected intracranially (right hemisphere) with HB1.F3-CD cells loaded or not with CRAd-S-pk7 and sacrificed at the indicated time points (n=3 per time point). *Bars: 400μm (H&E); 100μm (IHC). ND, none detected*

Table 1

Detection of infectious adenoviral progeny in animal tissues

Tissue	Sacrificed	Nude Mouse	Hamster	Cotton Rat
Serum	Day 1	NA	0/6	0/6
	Day 4	NA	0/6	0/6
	Day 7	NA	0/6	0/6
	Day 14	NA	0/6	0/6
	Day 30	NA	0/6	0/6
Right Hemisphere (Injected)	Day 1	NA	4/6	5/6
	Day 4	5/5	NA	NA
	Day 7	5/5	0/6	0/6
	Day 14	5/5	0/6	0/6
	Day 30	NA	0/6	0/6
Left Hemisphere (Non-Injected)	Day 1	NA	0/6	0/6
	Day 4	4/5	NA	NA
	Day 7	2/5	0/6	0/6
	Day 14	1/5	0/6	0/6
	Day 30	NA	0/6	0/6

Infectious adenoviral progeny was determined in the tissues of injected animals at the indicated time points. NA, means that such tissue was not available (NA) for the indicated animal at that specific time point.